https://doi.org/10.37434/tpwj2021.05.08

CALCULATION OF RESIDUAL STRESS-STRAIN STATE OF DEPOSITED STEEL SHEET PLATES

I.K. Senchenkov[1], **I.O. Ryabtsev**[2], **O.P. Chervinko**[1] and **A.A. Babinets**[2]
[1]S.P. Timoshenko Institute of Mechanics of the NAS of Ukraine
3 Nesterov Str., 02000, Kyiv, Ukraine
[2]E.O. Paton Electric Welding Institute of the NAS of Ukraine
11 Kazymyr Malevych Str., 03150, Kyiv, Ukraine. E-mail: office@paton.kiev.ua

Finite-element calculation procedure was developed and stress-strain and microstructural state was studied at single- and two-layer surfacing of 3 mm sheets from St3 steel by Sv-Kh19N18G6M3V2, PP-Np-25Kh5FMS and Sv-08A wires. Calculations of SSS, microstructural state and shape change of the sheets at surfacing under the smooth support conditions were performed. The model of plane-deformation state (PDS) predicts greater deflections, compared to the model of plane-stress state (PSS), except for materials with martensite transformations (PP-Np-25Kh5FMS). At surfacing by materials with martersite transformations, greater deflections are in place due to volumetric effects of transformation. Except for deposited metal with martensite transformations (25Kh5FMS), the model of simultaneous deposition of a layer predicts greater deflection, compared to that of bead-by-bead deposition and it can be used for assessment of upper deflection limit. Satisfactory correlation was obtained for calculated and experimental data on surfaced sheet deflections. Rational schemes of supporting and fastening the element edges were determined, which provide minimum residual deflections. Ref. 7, 1 Table, 7 Figures.

Keywords: arc surfacing, stress-strain state, surfaced sheet deformations, Bodner–Partom model, deflection calculation procedure

The work is devoted to development of a procedure of calculation of the current and residual stress-strain and microstructural state, as well as deflections of 3 mm steel sheets at deposition of steel layers with different structure and properties. Processes with single- and two-layer surfacing are considered. St3 sheets of 3 mm thickness surfaced by Sv-Kh19N18G6M3V2, PP-Np-25Kh5FMS and Sv-08A wires were selected as the objects of study.

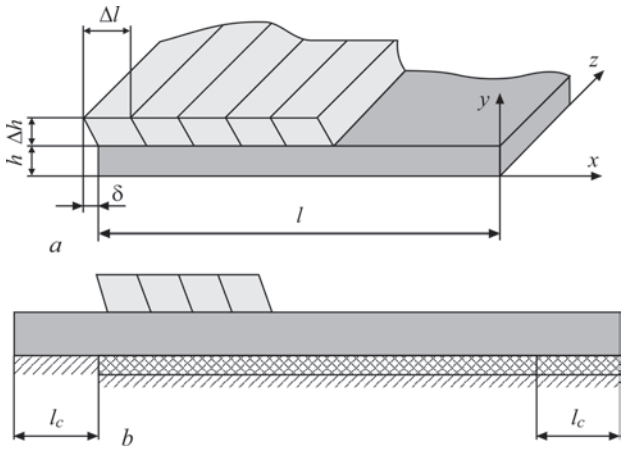

Figure 1. Scheme of deposition and shape of the beads (*a*) and conditions of fastening the side edges of the sheets during surfacing (*b*)

Figure 1 shows the scheme of deposition and shape of beads, as well as conditions of fastening the side edges of the sheets during surfacing, which were accepted when developing the calculation procedure. A scheme of rigid fastening of the sheet left edge and movable fastening of its right edge is considered. The following is assumed: l = 100 mm; h = 3 mm; Δh = = 2.4 mm, Δl = 5 mm, l_c = 25 mm. The bead deposition rate was 31 m/h. Sheet length along *Oz* axis was L = 200 mm.

The scheme of simultaneous (instantaneous) deposition of the bead in *Oz* direction is used in order to reduce the three-dimensional problem to a two-dimensional one. The task is now limited to the problem of plane deformation state (PDS) or plane stress state (PSS) in *Oxy* plane, depending on the conditions of fastening and supporting of the sheet.

At two-layer surfacing, the schemes of deposition of second layer beads without shifting (Figure 2, *a*) and with their 50 % shifting are considered (Figure 2, *b*). The scheme with sequential simultaneous deposition of applied metal layers with an interval, which is dictated by deposition conditions (Figure 2, *b*) is considered as the simplified one.

Experimental studies of deformation of 3 mm St3 steel sheets during surfacing were conducted by the following scheme. Surfacing with Sv-Kh19N18G-

I.O. Ryabtsev — https://orcid.org/0000-0001-7180-7782, A.A. Babinets — https://orcid.org/0000-0003-4432-8879

6M3V2 wire ensured producing deposited metal with an austenitic structure; with PP-Np-25Kh5FMS wire — martensitic-bainitic deposited metal with a small quantity of residual austenite; with Sv-08A wire — producing ferritic-pearlitic deposited metal, close in its chemical composition to base metal. Selection of exactly such surfacing materials is attributable to the difference in their physico-mechanical properties and structural state, compared to base metal, and, accordingly, to their anticipated different impact on the level of residual stresses and strains in the surfaced sheets.

So, at surfacing by Sv-Kh19N18G6M3V2 wire the level of deformations of St3 sheets will depend on the impact of local heating and considerable difference in the coefficient of thermal expansion (CTE) of the base and deposited metal. For PP-Np-25Kh5FMS wire it will depend on the impact of local heating and martensite transformation, which is accompanied by an increase of the deposited metal volume, as the difference in CTE is minimal in this case. At surfacing by Sv-08A wire the strain level will depend only on the impact of local heating, as there is practically no difference between the base and deposited metal in CTE and structural state.

Surfacing by all the wires was performed as individual beads with ≈ 50 % overlapping of the adjacent beads in the same mode: 150 A current; 22 V voltage; 31 m/h deposition rate. Such a surfacing mode provided a deposited layer ≈ 2.4 mm thick. Sheet surfacing was performed in one and two layers for each type of wire.

Sheets to be surfaced were fastened on the welding table with copper surface and were clamped to it using two steel straps in keeping with the design scheme: one of the straps pressed the sheet edge to the table, completely preventing its movement (rigid fastening), and the other did not allow the sheet edge deforming

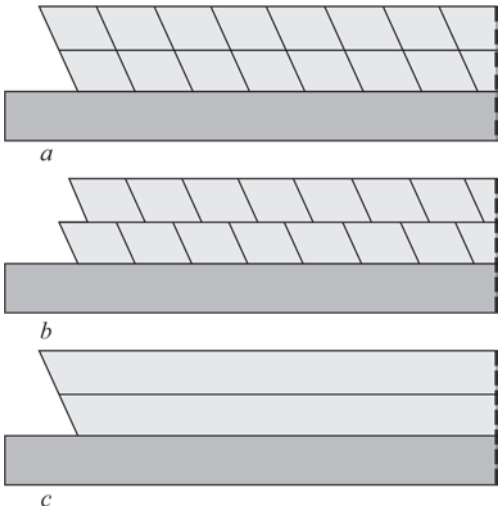

Figure 2. Scheme of two-layer surfacing of the sheets: *a* — without displacement of the second layer beads; *b* — with displacement of the second layer beads

in the vertical direction, but enabled its shifting in the horizontal plane (movable fastening) (Figure 3).

Surfacing of sheets with similar fastening, but with a gap between the sheets and the table was also performed. Surfacing of each sheet was begun from the side of rigid fastening and continued to the other edge without pauses for cooling. After surfacing of the entire sheet, the clamping strap was not removed up to its complete cooling.

Figure 4 shows the sheets after one-layer surfacing by three different wires.

At calculations bead deposition was modeled within a model of growing bodies [1]. This model uses nonclassical boundary conditions on the treated surface [2, 3].

Thermoviscoplastic behaviour of the base metal and deposited beads is described by Bodner–Partom model [4]. Model parameters, as well as thermophysical characteristics are specified using experimental data.

Microstructural transformations are modeled, using thermokinetic diagrams (TKD) of overcooled

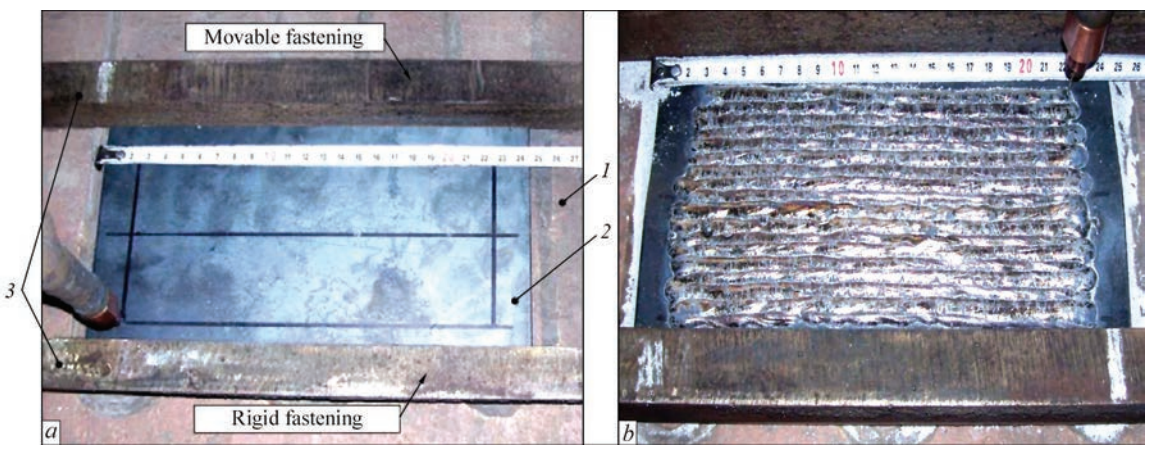

Figure 3. Method of fastening the sheets on the welding table (*a*): *1* — welding table with copper plate; *2* — sheet being surfaced; *3* — clamping straps; (*b*) — appearance of sheets after surfacing

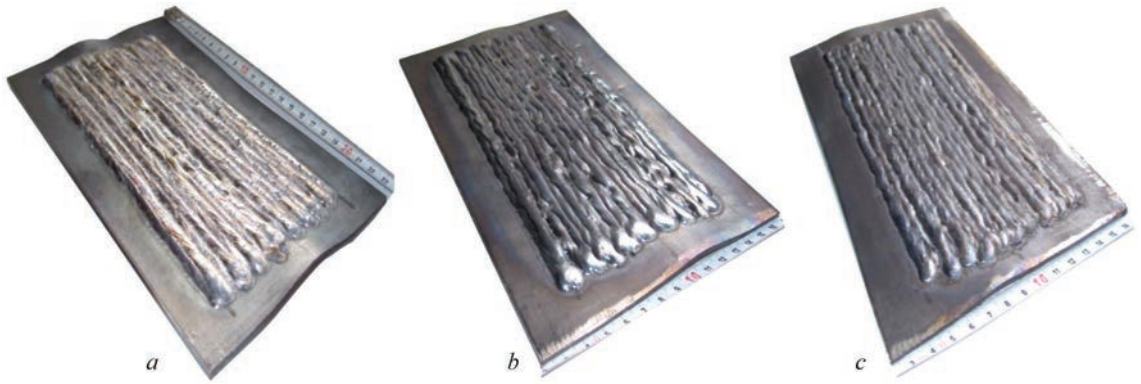

Figure 4. Appearance of deformed sheets after one-layer surfacing by the following wires: *a* — Sv-Kh19N18G6M3V2; *b* — Sv-08A; *c* — PP-Np-25Kh5FMS

austenite decomposition [5, 6]. For steels under consideration these diagrams were digitized for use in calculations.

Mathematical definition of the problem includes the following relationships:

• equations of equilibrium and heat conductivity

$$\mathrm{div}\,\underline{\sigma} = 0, \quad \overline{c}_v \dot{\theta} = \mathrm{div}(\overline{k}\,\mathrm{grad}\,\theta) + Q, \tag{1}$$

with thermal boundary and initial conditions

$$\begin{gathered} -k\,\vec{n}\,\mathrm{grad}\,\theta = -q + \gamma(\theta - \theta_C) + \sigma\varepsilon(\theta^4 - \theta_0^4); \\ \theta = \theta_0 \text{ at } t = 0; \end{gathered} \tag{2}$$

• determining equations

$$\varepsilon_{ij} = \varepsilon_{ij}^e + \varepsilon_{ij}^p + \varepsilon_{ij}^{\theta ph} + \varepsilon_{ij}^*, \quad \varepsilon_{kk}^p = 0; \tag{3}$$

$$\begin{aligned} s_{ij} &= 2G(e_{ij} - \varepsilon_{ij}^p - e_{ij}^{\theta ph} + e_{ij}^*), \\ \sigma_{kk} &= 3K_V(\varepsilon_{kk} - \varepsilon_{kk}^{\theta ph} - \varepsilon_{kk}^*); \end{aligned} \tag{4}$$

• flow equations

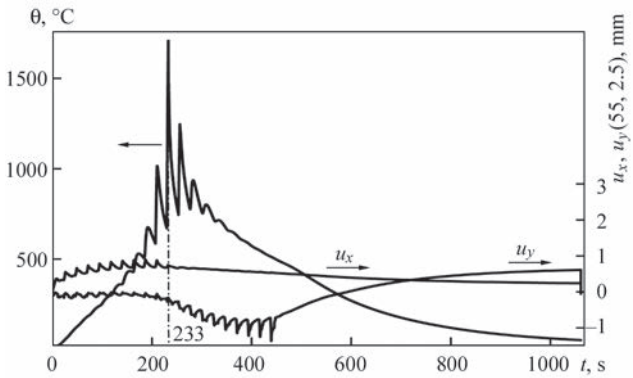

Figure 5. Temperature and movement of base point under the 11th bead in time. Surfacing with Sv-08A solid wire

$$\dot{\varepsilon}_{ij}^p = D_0 \exp\left\{-\frac{1}{2}\left[\frac{\left(\overline{K}_0 + K\right)^2}{3J_2}\right]^n\right\} s_{ij} \Big/ s_i, \tag{5}$$

$$\varepsilon_{ij}^p(0) = 0;$$

for base metal $\varepsilon_{ij}^*(0) = 0$;

• evolution equation for isotropic strengthening parameter

$$\dot{K} = m_1\left(\overline{K}_1 - K\right)\dot{w}^p, K(0) = 0, \tag{6}$$

where G, G_f and K_v, $K_{v,f}$ are the shear and bulk compression moduli; dash on top means calculation by the rule of mixture $\overline{(\bullet)} = (\bullet)_\xi C_\xi$, C_ξ are the volume phase concentrations, ξ = A, F, P, B, M of austenite, ferrite, pearlite, bainite and martensite, respectively; $K_{\xi 0}$, $K_{\xi 1}$, m_1, n, D_0 are the model parameters; $\dot{w}^p$ is the plastic power; s_i is the second invariant of the stress tensor; $\dot{w}^p = \sigma_{ij}\dot{\varepsilon}_{ij}^p$; $s_i^2 = 1/2 s_{ij} s_{ij}$; Q is the heat source; $\varepsilon_{ij}^*, \theta^*$ are the strains and temperature of element $\Delta v(t^*)$ at the moment of its build-up that ensure conditions $\sigma_{ij}(\varepsilon_{ij}^*, \theta^*) = 0$ in $\Delta v(t^*)$ at build-up moment $t = t^*$, k and $\overline{c}_v$ are the coefficients of heat conductivity and volumetric heat capacity; $\varepsilon_{ij}^{\theta ph}$ is the thermal phase strain.

Mechanical boundary conditions are specified by those of surfacing and fastening of the element.

The problem of thermomechanical state of the surfaced parts is solved numerically by finite element method [7]. An eight-node rectangular finite element is used. Nonstationary equations are integrated by implicit time-stepping schemes with variable integration step. Iteration processes at each step are accelerated using Stephenson–Aitken procedure.

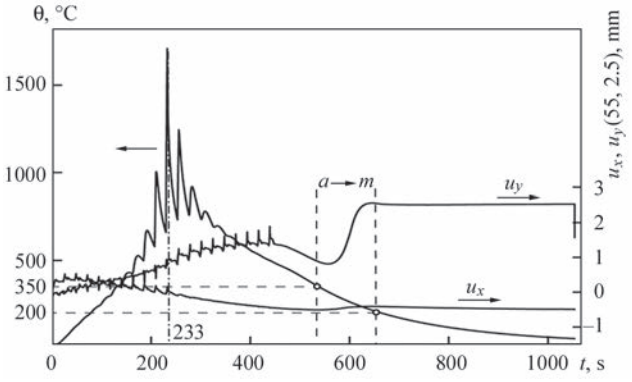

Figure 6. Temperature and movement of base point under the 11th bead in time. Surfacing by PP-Np-25Kh5FMS flux-cored wire

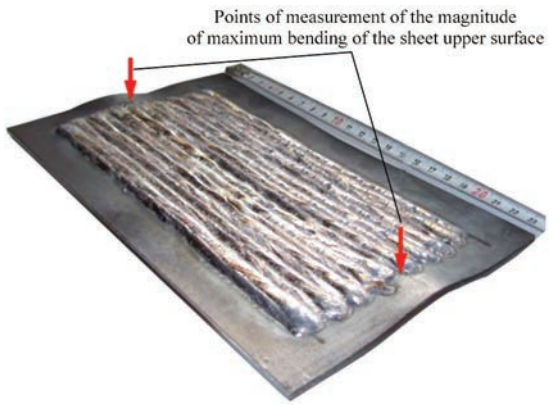

Figure 7. Scheme of measurement of the magnitude of sheet deformation after surfacing

Influence of martensite transformation on the kinetics of temperature and movements under the conditions of surfacing with a gap between the sheet and support is illustrated in the point in the base material under the 11th bead, which is deposited at moment of time t_{11} = 2.33 s. Such curves are given in Figure 5 for surfacing with Sv-08A wire and in Figure 6 for the case of surfacing by PP-Np-25Kh5FMS wire.

In the second case, an essential increase of deflection in the area of martensite transformation is in place. Points on the temperature curve in Figure 6 indicate the moments of entering the region of austenite-martensite transformation and leaving it. Dashed curves limit this area on axes θ and *t*. Instantaneous change of deflection at $t \approx 1100$ °C corresponds to releasing the right edge of the sheet from smooth fastening.

Experimentally, the characteristic deflections of the surfaced sheets were determined as follows. After cooling down and releasing of the fastened edges, the sample was placed on a smooth plate and normal displacement of the sheet upper surface relative to the plate was measured by an indicator. The maximum local value of the above-determined deflection in the cross-section of the surfaced part of the sheet was taken as the characteristic deflection (Figure 7). With such a definition the characteristic deflection is always positive.

For three Sv-Kh19N18G6M3V2, PP-Np-25Kh5FMS and Sv-08A wires the experimental and calculated data for the characteristic deflections at one-layer surfacing under the conditions of smooth support are given in the Table.

As one can see from the tabulated data, PDS model predicts greater deflections, compared to PSS model, except for materials with martensite transformations (25Kh5FMS). At deposition of materials with martensite transformations greater deflections are in place, because of bulk transformation effects. It should be also noted that much greater deformations are observed at surfacing with a gap between the sheet and the welding table, than in the case of tight pressing of the sheet to the table.

Similar calculations were conducted for the case of two-layer surfacing. In particular, at calculation of two-layer surfacing by Sv-08A solid wire the following results on deflections were obtained under the conditions of smooth support: schemes without bead overlapping (Figure 2, *a*) — 1.02 mm for PDS model, and 0.91 mm for PSS model. The scheme of sequential simultaneous deposition of the layers yields the following deflection values: 1.00 mm for PDS, and 0.91 mm for PSS. Experimental values of deflection were 0.8 mm. Results of calculation of the deflections for the case of bead deposition with overlapping and without overlapping coincide with less than 10 % discrepancy.

Experimental and calculated data on deflection of sheets (mm), surfaced by different wires in one layer*

Supporting conditions	PDS/PSS	Surfacing materials								
		Sv-Kh19N18G6M3V2			PP-Np-25Kh5FMS			Sv-08A		
		1	2	3	1	2	3	1	2	3
Smooth	PDS	1.45	1.61	0.7	1.52	1.69	1.7	1.21	1.22	0.7
	PSS	1.34	1.38		1.93	1.72		1.13	1.12	
With a gap	PDS	2.77	2.18	2.0	2.81	4.96	2.5	2.84	2.27	1.2
	PSS	2.66	1.68		2.55	4.22		2.35	1.69	

Notes. *Columns with numbers 1 and 2 correspond to calculated data at simultaneous and bead-by-bead deposition, respectively. PDS and PSS lines correspond to calculation models. No.3 columns correspond to experimental data. Deflections are determined after cooling and releasing the edges.

Discrepancy of the given calculated and experimental results is determined, on the one hand, by inaccuracy of the mathematical model in terms of ignoring the contact interaction of the sheet with the supporting surface, and on the other hand — by technical difficulties in ensuring experimental studies under all the conditions of fastening the sheet edges.

Conclusions

1. The numerical finite-element procedure for calculation of the current and residual stress-strain and microstructural state of surfaced sheets was improved, in order to take into account the conditions of their fastening during surfacing.

2. Calculations of SSS, microstructural state and change of the shape of the sheets at surfacing under the conditions of smooth support were performed. It is found that these conditions provide a smaller residual deflection, compared to those of the free boundary on the element lower surface. Influence of the conditions of element fastening on the maximum values of residual deflections, as well as of the effect of microstructural transformations in the deposited metal was assessed.

3. PDS model predicts greater deflections, compared to PSS model, except for materials with martensite transformations (25Kh5FMS). At deposition of materials with martensite transformations greater deflections are found due to the bulk effects of transformation.

4. Except for the deposited metal with martensite transformations (25Kh5FMS), the model of simultaneous deposition of a layer predicts greater deflection, compared to the model of bead-by-bead deposition, and it can be used for assessment of the upper deflection boundary.

5. Calculation results satisfactorily correlate with the experimental data.

1. Senchenkov, I.K. (2005) Thermomechanical model of growing of cylindrical bodies from nonlinear materials. *Prikl. Mekhanika*, 41(**9**), 118–126 [in Russian].
2. Ryabtsev, I.A., Senchenkov, I.K., Turyk, E.V. (2015) *Surfacing. Materials, technologies, mathematical modeling.* Gliwice, Silesia Polytechn. In-te, 44–100 [in Polish].
3. Ryabtsev, I.A., Senchenkov, I.K. (2013) *Theory and practice of surfacing works.* Kyiv, Ekotekhnologiya [in Russian].
4. Bodner, S.R. (2000) *Unified plasticity — an engineering approach.* Final Rep. Technion. Israel Inst. of Tech., Haifa.
5. Popov, A.A., Popov, A.E. (1961) *Isothermal and thermokinetic diagrams of overcooled austenite decomposition:* Refer. Book of heat-treater. Moscow-Sverdlovsk. GNTI Mashlit [in Russian].
6. Shorshorov, M.Kh., Belov, V.V. (1972) *Phase transformations and change of steel properties in welding*: Atlas. Moscow, Nauka [in Russian].
7. Motovilovets, I.A., Kozlov, V.I. (1987) *Mechanics of related fields in materials and structure elements.* In: 5 Vol., Vol. 1: *Thermoelasticity*. Kiev, Naukova Dumka [in Russian].

Received 19.04.2021